TRIBOLOGY TRANSACTIONS
2025, VOL. 68, NO. 1, 28–38
https://doi.org/10.1080/10402004.2024.2431523

Experimental Study of the Effect of Thickener on the Film Thickness in the Contacts of a Grease-Lubricated Ball Bearing at Low Speed

Michal Okal[a], David Kostal[a], Jude A. Osara[b], Piet M. Lugt[b,c], Ivan Krupka[a], and Martin Hartl[a]

[a]Faculty of Mechanical Engineering, Brno University of Technology, Brno, Czech Republic; [b]Faculty of Engineering Technology, University of Twente, Enschede, The Netherlands; [c]SKF Research and Technology Development, Houten, The Netherlands

ABSTRACT

The level of starvation in axially loaded grease lubricated ball bearings can be well described by the product of the base oil viscosity, the half contact width and the rotational speed (ηbu). This paper highlights the effect of the thickener as another parameter for estimating the film thickness in a ball bearing. Film thickness measurements were done with an optical simulator of the ball-on-disc configuration and a real ball bearing using the capacitance method. Three greases with the same base oil but different thickener types were selected for the experiments. Two greases followed the ηbu model but the grease with alicyclic di-urea thickener produced a higher thickness than the model prediction, which is most likely caused by the formation of residual layers on the contact surfaces. The layer formation occurs in the first few hours of operation reaching a thickness of about 500–550 nm. Other greases also form layers, but they are comparable to prior observations, and they follow the model. The evolution of the normalized film thickness versus ηbu in the case of alicyclic-di urea grease shows the same trend as the other grease types but with overall higher values.

ARTICLE HISTORY
Received 8 July 2024
Accepted 14 November 2024

KEYWORDS
EHL: grease; thickener; ball bearing

Introduction

Most rolling bearings today are lubricated with greases and, in contrast to oils, the lubrication mechanisms of greases are not entirely clear. To predict the performance, it is important to calculate the lubricating film at the rolling bearing contacts. This film has a major effect on the friction of the bearing and also on its overall life. If the grease no longer separates the contact surfaces, bearing life is shortened. The lubrication regime is elastohydrodynamic lubrication (EHL), where the film thickness can be predicted using the Hamrock Dowson equation (*1*) or the Nijenbanning equation (*2*). These equations consider only fully flooded conditions where there is an unlimited amount of lubricant in the inlet of the contacts. However, in normal operation of bearings lubricated with grease, starved contacts are more common. Starvation is characterized by a limited amount of available lubricant leading to a reduced film thickness.

Grease lubrication in rolling bearings is complex because of the complex rheological properties of greases (*3*). Greases are composed of a base oil, thickener, and additives. Grease lubrication in rolling bearings can be divided into several phases with the churning phase occurring during the first part of the operation, when the lubricant is redistributed through the bearing and grease reservoirs are formed. After that, a small amount of lubricant remains on the tracks to lubricate the individual contacts. Then comes the bleeding phase where the amount of lubricant available is determined by the feed and loss balance (*4*). This phase persists until the end of the grease life (*5*). The length of the churning phase depends on the rheological properties of the individual grease samples. The amount of base oil released from the thickener structure during bearing operation is determined by the bleeding rate, which should not be too large for long lubricant life. After a certain period of time, the bleeding rate of grease decreases and the amount of oil available for lubrication decreases leading to an increase in contact starvation.

One of the first published papers on the topic of starvation in EHL contacts was by Wedeven et al. (*6*). They described the formation of the meniscus in the inlet of the contact and its impact on the lubricating film in the contact. This work was extended by Kingsbury (*7*) who introduced the concept of parched lubrication: a condition where there is a minimal amount of oil available and where the film thickness is almost equal to the inlet layer thickness. This state is accompanied by the lowest possible rolling friction. In recent years, Chevalier et al., (*8*) Damiens et al., (*9*) and Venner et al. (*10*) have made significant progress in describing the starved EHL point contacts using the Elrod algorithm. It was shown that the central film thickness depends

CONTACT Michal Okal Michal.Okal@vut.cz
Review led by K. Feng.
This article has been corrected with minor changes. These changes do not impact the academic content of the article.

on the lubricant layer thickness at the inlet of the contact and the number of overrollings. This has been experimentally verified by Svoboda et al. (*11*) on a tribometer of ball-on-disc configuration with multiple rolling elements. Van Zoelen et al. (*12*) extended the work further and considered replenishment caused by centrifugal forces.

To measure the thickness of the lubricating film in rolling bearings, the electrical capacitance method is used. The EHL elliptical contact between the ball and bearing ring mimics a parallel plate capacitor, where the thickness of the lubricating film determines the magnitude of the capacitance. The capacitance method has been used many times, for example by Jablonka et al., (*13*) Bader et al., (*14*) and Zhang and Glovnea (*15*). Cen and Lugt (*16,18*) and Cen et al. (*17*) used the method to determine the key parameters influencing the thickness of the film in the contact. The relative film thickness h_g/h_{ff} in an axially loaded radial ball bearing was described by an equation based on the product of half contact width b, velocity u, and base oil viscosity η (*16*):

$$h_g/h_{ff} = 8.294 \times 10^{-4} \times (\eta b\ u)^{-0.791} \quad [1]$$

A further extension of the method was done by Shetty et al. (*19*) who improved the method by developing a full electrical model of the bearing, including the dielectric constant. The method has been successfully used to investigate the effects of vibration (*20*) and the amount of grease applied (*21*) on the thickness of the lubricating film in a ball bearing.

The second method for studying the lubrication of greases is via a ball-on-disc tribometer. Cann (*22*) showed a significant effect of thickener on the film thickness under starvation conditions. She measured the film thickness of grease lubricants and found that the thickener contributed to the overall film thickness. Cann (*23*) showed that the thickener also enters the contact by measuring the residual film after stopping the ball-on-disc set-up. The contribution of the thickener was also shown under fully flooded conditions, where the film formed by the grease was thicker than that formed by the base oil alone. Another important study by Cann (*24*) with three greases with the same base oil but different thickener type showed a strong effect of thickener type on film thickness and friction. Tetra-urea greases produced thicker thickener layers on the track than lithium greases. Kaneta et al. (*25*) focused mainly on polyurea greases and compared the effect of different thickener structures (aliphatic, aromatic and alicyclic) on film formation. It was shown that aliphatic thickener forms thicker films than aromatic or alicyclic thickener. An increase in the concentration of thickener in the EHL contact and hence film thickness was also shown by Hoshi et al. (*26*). The effect of shear has also been investigated and it has been shown that shear reduces the thickener layer on the surfaces. The connection between the thickener contribution to the lubricating film, friction and torque in a ball bearing was presented by Kanazawa et al. (*27,28*). A good correlation between the behavior on the ball-on-disc tribometer and the actual rolling bearing could be seen. The contribution of the thickener of mechanically aged grease to the lubricating film was further studied by Cen et al. (*29*). They showed that mechanical degradation reduces the ability of the thickener to increase the lubricating film.

It can be seen that there is still a difference between the film thickness measured on the ball-on-disc tribometers and the film thickness in real rolling bearings. There are only a small number of publications that systematically compare the results from both approaches. Therefore, it is still unclear whether the thickener's contribution to the lubricating film observed in a single EHL contact can be applied to a real rolling bearing. This paper helps to address these questions and fill the knowledge gap by investigating the lubricating film thickness on both a ball-on-disc tribometer and a real rolling bearing under the same running conditions and with identical greases. Model greases containing the same base oil but different thickeners are used for the experiments. A direct comparison of the rolling bearing measurements with equivalent thickness measurements in a tribometer with a ball-on-disc configuration will show the interconnectedness of the two systems. The presented results provide insight into the influence of grease composition on the determination of film thickness in a rolling bearing, primarily at low speeds.

Materials and methods

This paper mainly focuses on the comparison of two experimental approaches. A standard optical tribometer of ball-on-disc configuration was used, allowing direct insight into the contact area. The second device was a rolling bearing test rig allowing the measurement of the real lubrication film thickness in a radial ball bearing using the electrical capacitance method.

Ball-on-disc tribometer

In-situ measurements were performed on a ball-on-disc device. A schematic of the device is shown in Fig. 1. In this setup, a circular EHL contact is made between the ball and the transparent glass disc. The 25.4 mm diameter ball was made of 100Cr6 bearing steel. The transparent disc was made of borosilicate glass (BK7). The modulus of elasticity of the 100Cr6 bearing steel was 210 GPa and the modulus of elasticity of the BK7 borosilicate glass was 81 GPa. The surfaces of both elements were optically smooth (Ra $<$ 6 nm) and the experiments were performed under clean rolling conditions. The ball and disc were independently driven by servo motors and the load in contact was created by a dead weight-and-lever system. The transparent disc allows direct insight into the contact area facilitating the measurement of the lubrication layer thickness. The film thickness measurement was recorded using a microscope with a high-speed CMOS camera.

Colorimetric interferometry was chosen as the observation method (*30*). The method is based on the interference of incoherent white light that occurs between two rays reflected from the bottom surface of the disc and the surface

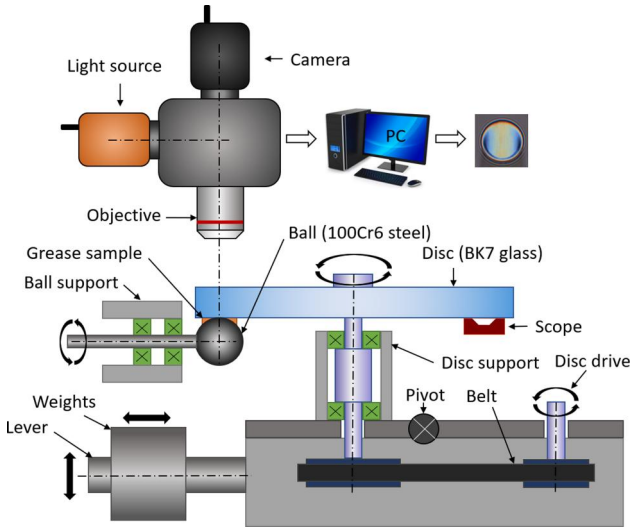

Figure 1. Scheme of the ball-on-disc test rig.

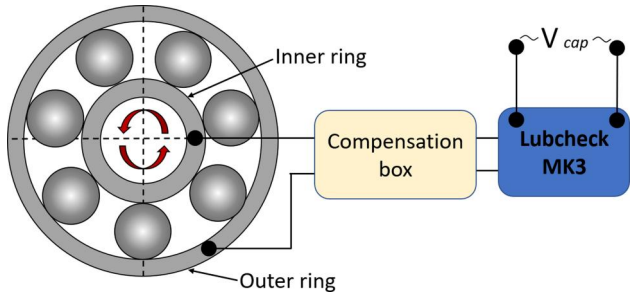

Figure 2. Scheme of the ball bearing test rig.

of the ball. The reflectivity of the underside of the disc is enhanced by a chrome coating. The subsequent calibration of the method consists in taking a monochromatic and a chromatic image of the same static contact. This is followed by the assignment of a color-specific thickness. The method is described in detail by Hartl et al. (*31*). For measuring higher thickness, a trichromatic source range can be used, which contains the light of three diodes. The sources create a light intensity of a specific wavelength and enable a much larger range of interference measurements. The range can then be used up to a thickness of 1500 nm. The range when using white light enables measurements up to a thickness of 900 nm.

Ball bearing test rig

The second device used in this study was a bearing test rig developed to measure the film thickness in a deep groove ball bearing *via* the electrical capacitance method of Heemskerk et al. (*32*). A scheme of the device is shown in Fig. 2 and a description of the device can be found in Cen and Lugt (*33*). In this paper, we used a 6209-2Z ball bearing with rubber shields. The stationary outer ring of the bearing is located in the house and connected to the "Lubcheck Mk3" apparatus. The bearing was loaded axially by a pneumatic actuator. The measured bearing capacitance is converted to an output voltage Vcap, by the Lubcheck Mk3, that is recorded in real time. The recorded voltage is therefore a measure of the film thickness between the inner and outer rings. Subsequent, calibration is carried out with bled oil under fully flooded conditions, where the film thickness can be easily calculated (via the Hamrock and Dowson equation) using the viscosity. The bled oil was obtained by centrifugation from the test samples and was filtered through filter paper to remove potentially remaining thickener particles. The bled oil has been shown to have a very similar dielectric constant as the grease (10%) (*34*). Five milliliters of bled oil was put into the bearing for a calibration measurement in the speed range of 120–700 rpm and at a load of 200 N during which the Lubcheck signal Vcap was recorded. Subsequently, the measured values were related to the Hamrock and Dowson calculated lubricant film thickness (*1*,*35*). More information about the calibration and the test method can be found in Shetty et al. (*19*) and Cen and Lugt (*33*).

Samples and test conditions

For the experiments, greases with Poly-alpha-olefin (PAO) base oil were used. The grease samples did not contain any additives. Three types of thickeners were used, namely, alicyclic di-urea, lithium complex, aliphatic-di-urea. Table 1 lists the properties of the test greases.

The bleeding ratio of grease samples was evaluated using the static oil separation test in accordance with DIN 51817 (*36*). Grease samples weighing 30 g were placed in a conical sieve and subjected to a load generated by a 100-g weight. The tests were conducted for 48 h at 60 °C. Afterward, the separated oil was weighed, and the bleed ratio was calculated by dividing w_o by w_g, where w_o is the weight of the separated oil and w_g is the weight of the grease sample tested.

Film thickness measurements using optical EHL rig

The thickness of the lubricating film between the ball and disc was measured at three speeds under pure rolling and fully flooded conditions. Grease was continuously pushed into track using a scoop. The test speed was 330 mm/s, 550 mm/s, and 826 mm/s at room temperature of 24 °C. In all tests, the maximum Hertzian pressure was 0.9 GPa. The total duration of the experiments was 7 h. After the experiments were completed, the motors were stopped and the static contact thickness was measured at 4 locations on this disc. The results from the static contact were compared with the images of the static contact taken before the start of the experiment.

Film thickness measurements using ball bearing test rig

All lubricants were tested with the same ball bearing to minimize scatter in measurement results due to potential differences in bearing dimensions/properties. Two types of experiments were conducted. The first consisted of filling the bearing with fresh grease for each speed tested. The second type of experiment involved a one-time filling of the bearing, where the bearing was first put through a 24-h run-in phase at 4000 rpm. Then the bearing was stopped and the

Table 1. Properties of all three greases used in this study.

Grease property	(Alic.) Grease	(Lith.) Grease	(Alip.) Grease
Base oil type	Poly-alpha-olefin (PAO)	Poly-alpha-olefin (PAO)	Poly-alpha-olefin (PAO)
Viscosity of base oil ($mm^2 \cdot s^{-1}$) at 40 °C	46	46	46
Thickener type	Alicyclic di-urea	Lithium complex	Aliphatic di-urea
Thickener concentration (wt%)	15	16	15
Penetration (60 W)	275	268	221
Density of the grease (g/cm^3)	0.85	0.85	0.84
Static oil bleeding ratio W_o/W_g (%)	4.8	3.2	3.4

measurement test was started from the lowest speed to the highest speed. The grease volume in the bearing was equal to 30% of the bearing free volume. The film thickness measurements were then carried out at room temperature of 24 °C and an axial load of 200 N. The load produces a maximum contact pressure of 0.9 GPa. The bearing experiments were carried out in the range of 120 rpm to 700 rpm. The rotational speeds of 120, 200, and 300 rpm are equivalent to contact linear speeds of 330 mm/s, 550 mm/s, and 826 mm/s, respectively (therefore, similar to the ball-on-disc experiments). The tested range of 120, 200–700 rpm corresponds to ndm (speed times mean diameter of the bearing) values of 10,200, 17,000, and 60,000 mm/min, which can be characterized as "low speed" (*37*). The length of each experiment done at a specific speed was 24 h. Both the measured grease film thickness (h_g) and calculated fully flooded film thickness(h_{ff}), based on the velocity, viscosity of the base oil, and temperature were averaged over 24 h. The Hamrock and Dowson equation and Walthers' equation were used for the calculations. The quotient of both values is the normalized film thickness (h_g/h_{ff}).

Results

Ball-on-disc tribometer

Figure 3 shows the thickness evolution at constant velocity under fully flooded conditions for (Alic.) grease. The theoretical values of film thickness for given speeds for the base oil were added to the graph. The Hamrock and Dowson equations were used to calculate the film thickness (*1*). At the early stage of the experiment, 0.01 h, the thickness was significantly larger than for the following 0.1 h. This applies to all speeds. Figure 4 shows images of typical interferograms from these experiments. These measurements show that, for velocities of 550 mm/s and 826 mm/s there was a loss of color saturation indicating the limit of the method. The interferograms show that the minimum in film thickness at time 0.1 h, is caused by a minimization of the thickener effect. The increase in film thickness (after 0.1 h) in Fig. 3 is reflected in the interferograms by a gradual change in color. The color change corresponds well with the color gamut obtained from the calibration. For all three velocities, there was an increase of approximately 250 nm in thickness between time 0.1 and 5 h during the experiment. After a time of about 5 h of the experiment, a stabilization of the values was observed. At 826 mm/s, the light source was changed from white light to a trichromatic light source. This was to increase the range of measurable thickness during the experiment. The change affected the hue of the

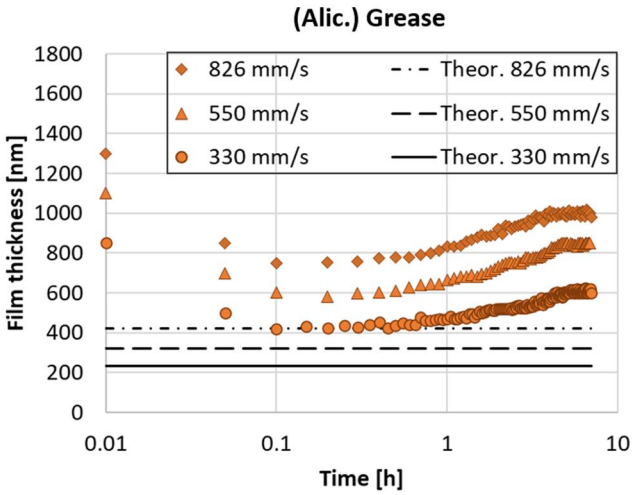

Figure 3. Fully flooded film thickness of (Alic.) grease.

interferograms and the colors, Fig. 4 interferograms at fully flooded conditions for (Alic.) grease (speed 330 mm/s, 550 mm/s and 826 mm/s). Between 0.1 and 5 h, the shape of the interferogram changed for all three velocities. At time 0.1 h, the minimum thickness has a horse-shoe or U-shape. Subsequently, the central part of the area narrowed and a change from a rounded shape to an edge shape was observed at the outlet. For a speed of 330 mm/s, the edge was observed at the minimum thickness at 5 h of the experiment, for a speed of 550 mm/s, at 4 h of the experiment, and for 826 mm/s, at 3 h of the experiment.

Figure 5 shows the results from the experiment with (Lith.) grease. At 0.01 h, the film thickness was the highest of the entire experiment for all the speeds. In Fig. 6 it can be seen that the interferograms of the contact show that the effect on film thickness of the entering thickener particles is less pronounced than in the case of the (Alic.) grease. Particles were mostly observed at 330 mm/s, even after 1 h of experiment. In the following hours, however, no particles were observed. Between 0.01 and 0.1 h of the experiment, a slight decrease in thickness was observed. For all velocities, the decrease was around 50 nm which was reflected in the change of color of the interferogram. Between 2 h and 5 h, the values stabilized. No further change in the shape of the thickness distribution or change in the color of the interferogram was observed, similar to the case of (Alic.) grease.

Figure 7 shows the evolution of the film thicknesses for (Alip.) grease and Fig. 8 shows the interferograms from the experiments. (Alip.) grease shows the same evolution as (Lith.) grease, with the thickness higher in the early moments of the experiments followed by a decrease and

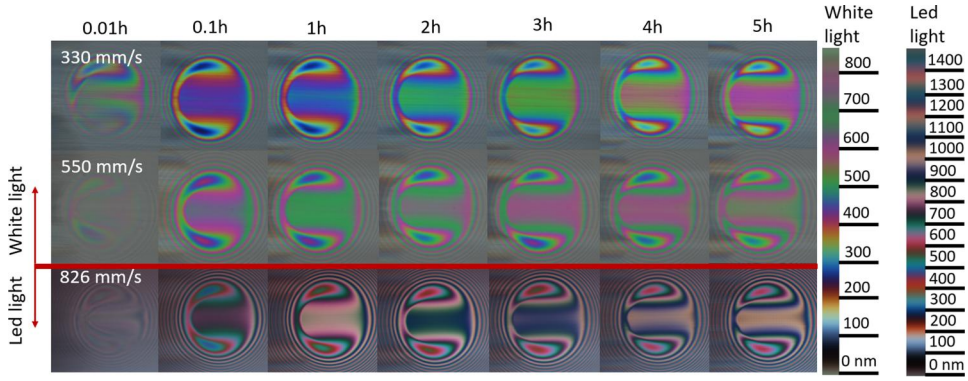

Figure 4. Interferograms at fully flooded conditions for (Alic.) grease (speed 330 mm/s, 550 mm/s, and 826 mm/s).

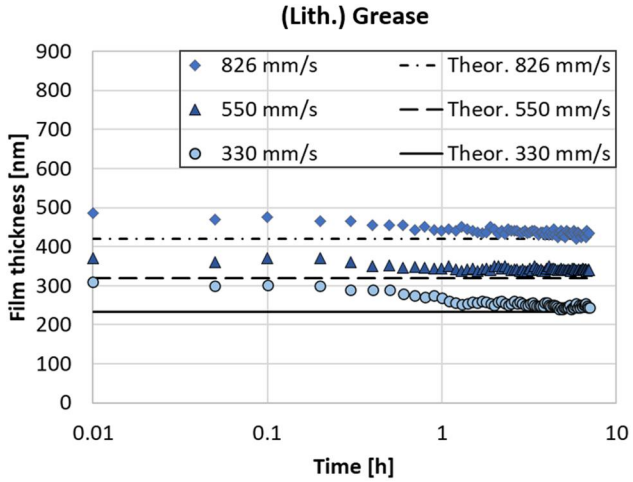

Figure 5. Fully flooded film thickness of (Lith.) grease.

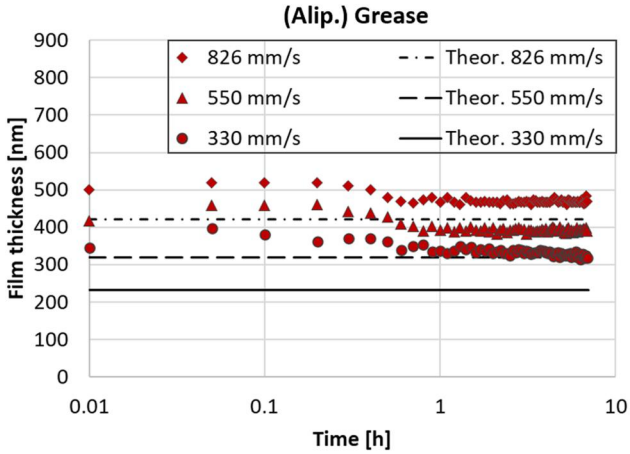

Figure 7. Fully flooded film thickness of (Alip.) grease.

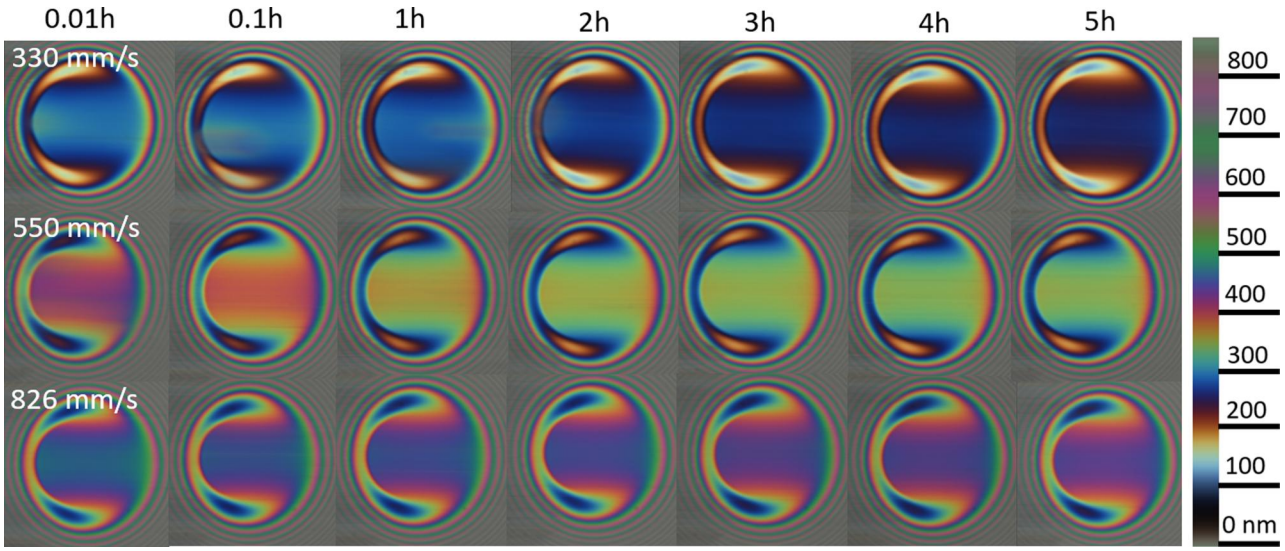

Figure 6. Interferograms at fully flooded conditions for (Lith.) grease.

stabilization after about an hour. The decrease was by about 50 nm, similar to the previous case. Comparing with (Lith.) grease, the thicknesses for all three velocities were larger here. (Alip.) grease gave 70–90 nm thicker films for the same velocity than were found for (Lith.) grease. No change in the shape of the minimum thickness as in the case of (Alic.) grease was observed.

Figure 9a shows interferograms of static contacts before and after the experiments that were done at 550 mm/s running for 7 h. For all the grease types, it can be seen that the contact is grey at the start of the experiment, indicating a thickness close to zero. For (Alic.) grease, small particles of thickener can be seen around the edges (white circle). Small particles can also be seen in the case of (Lith.) grease. The difference between

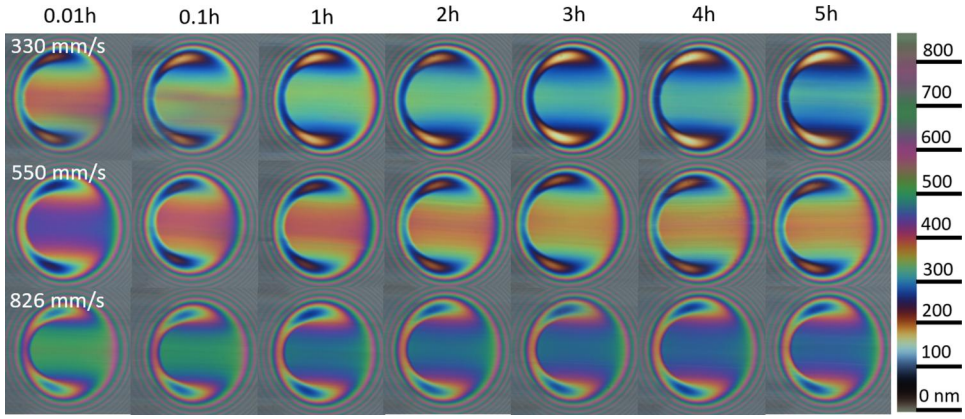

Figure 8. Interferograms at fully flooded conditions for (Alip.) grease.

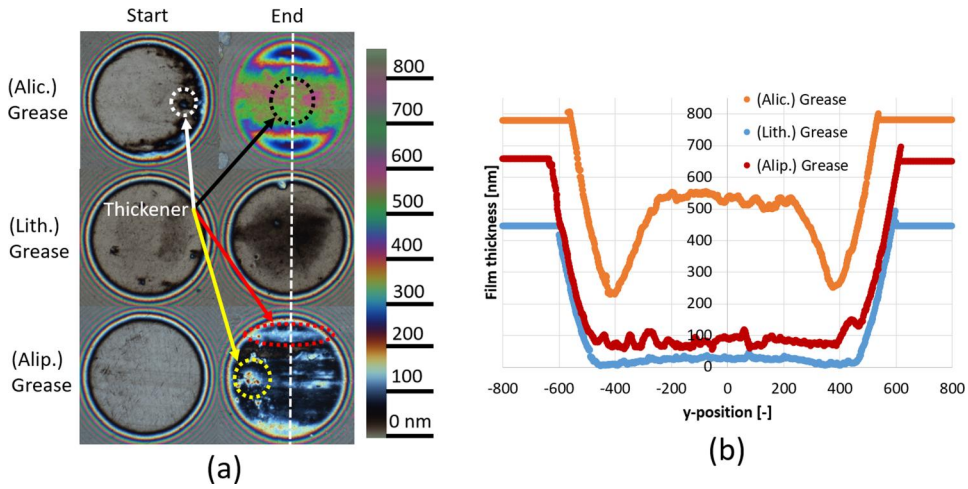

Figure 9. (a) Comparison of interferograms and (b) film cross section profiles of the static contacts before and after the experiment at 550 mm/s.

the samples is pronounced at the end of the experiment. (Alic.) grease shows the highest film thickness in the central region (black circle), what in Fig. 9b is a cross section taken shows a thickness between 500 and 550 nm. The interferogram clearly shows the minimum thickness which was 240–260 nm. The shape of the cross-section shows that the thickener adhered unevenly and the horseshoe-shaped region of minimum thickness Fig. 4 is not so favorable for thickener adhesion. For (Alip.) grease, one can see a slight swell compared to the beginning of the experiment of about 20–30 nm in the central region. For (Alip.) grease there was an increase in thickness to 70–110 nm. In all cases, the film thickness shapes show the formation of agglomerates. For (Alic.) grease, these agglomerates were more particle-like (white and black circle). In (Alip.) grease, they were also particulate (yellow circle) but can seem to be more elongated in the rolling direction (red circle).

Real ball bearing measurement

Figure 10 shows the evolution of the film thicknesses for the tested greases in the real bearing for different speeds. Directly measured film thickness values (h_g) are shown in addition to values calculated assuming that the bearing is lubricated by the base-oil under fully flooded conditions (base oil film thickness) (h_{ff}). An increase in calculated base oil film thicknesses with increasing speed is evident despite the increasing temperature and therefore decreasing viscosity. However, the behavior of the grease film thickness for the various greases was quite different. (Alic.) grease showed the highest values, with a thickness of approximately 600 nm at 330 mm/s. Increasing the velocity led to an increase in thickness only up to 1100 mm/s after which a slight decrease was observed for all greases. The same trend was observed, where an increase in thickness due to velocity was observed up to a velocity of 1100 mm/s but the film thickness varied between samples. At a speed of 330 mm/s, the thickness was 280 nm for (Lith.) grease and 360 nm for (Alip.) grease. The difference in film thickness between the samples was also observed at the highest speed of 1800 mm/s where (Alic.) grease showed a thickness of 680 nm, (Lith.) grease 320 nm and (Alip.) grease 390 nm. (Alic.) grease gave the largest spread in film thickness. (Lith. And Alip.) greases gave significantly smaller deviations, approaching the deviations of the h_{ff} calculation. The temperatures of all three samples were always similar, see Fig. 10 very small variations could be ascribed to temperature variations in the laboratory.

Figure 11 shows the evolution of the normalized thickness versus the product of base oil viscosity, half-contact width and velocity (ηbu). The normalized film thickness is the ratio between the measured grease film thickness h_g and the calculated fully flooded base oil film thickness h_{ff}. For

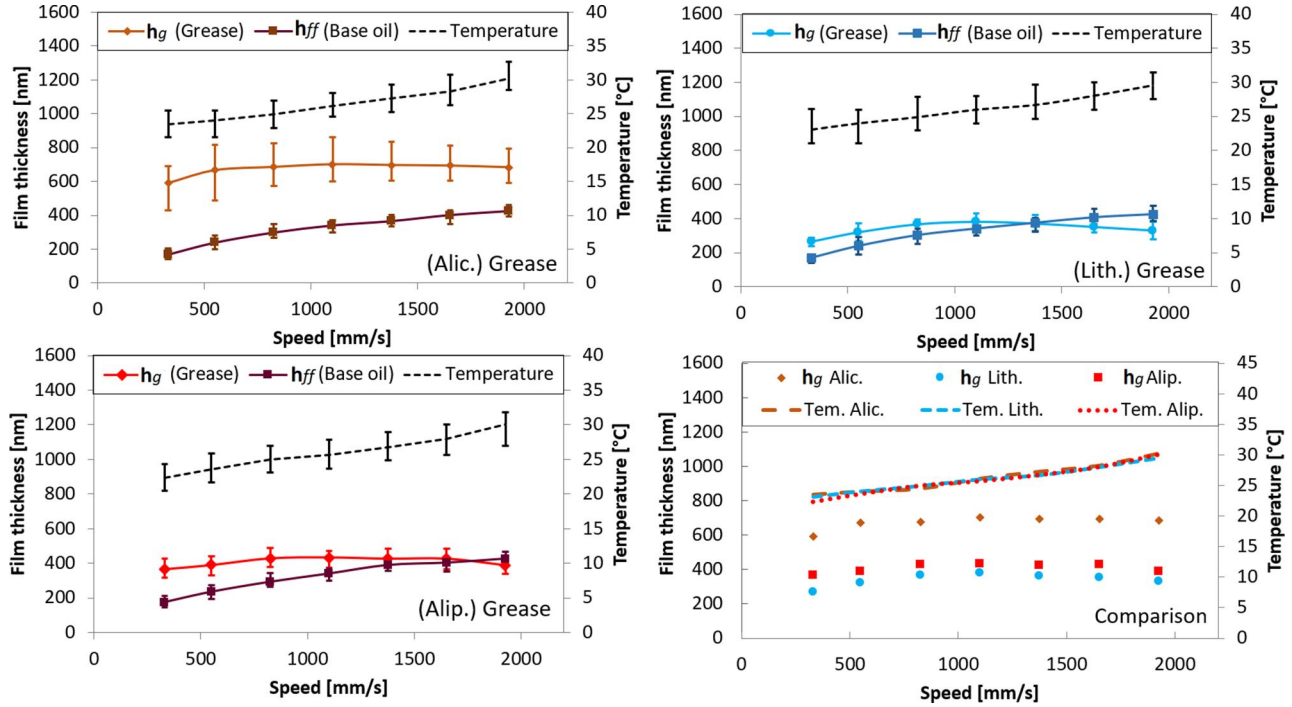

Figure 10. Film thicknesses in the 6209 ball bearing for tested greases with axial load 200 N.

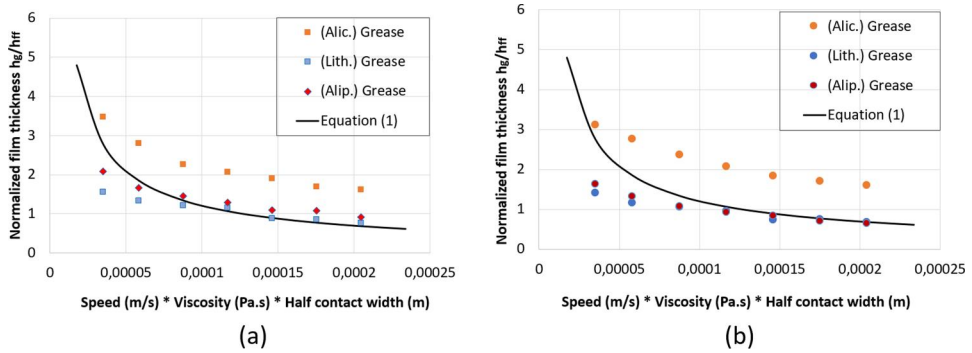

Figure 11. Relationship between normalized film thickness h_g/ h_{ff} and η b u: (a) each point with fresh grease, (b) one fill for all points, after run-in.

Fig. 11a, fresh grease was always used for each measured point and for Fig. 11b, the same grease filled in the bearing was used for all the points per grease. The measurements are compared to Eq. [1], the power fit film thickness equation from Cen and Lugt (*16*,*18*,*33*). It should be noted that Cen and Lugt (*16*) fitted a simple exponential equation that made it possible to illustrate the effects of speed and viscosity for a wide operational domain but that the equation did not perfectly fit the measurements at very low speed. It can be seen that (Lith.) and (Alip.) greases follow Eq. [1] quite well, particularly for $\eta bu > 0.0007$ but that the alicyclic di-urea thickened (Alic.) grease gives significantly larger values of normalized thickness (*33*). This is consistent with the ball-on-disc experiments where this alicyclic di-urea grease also showed thick films.

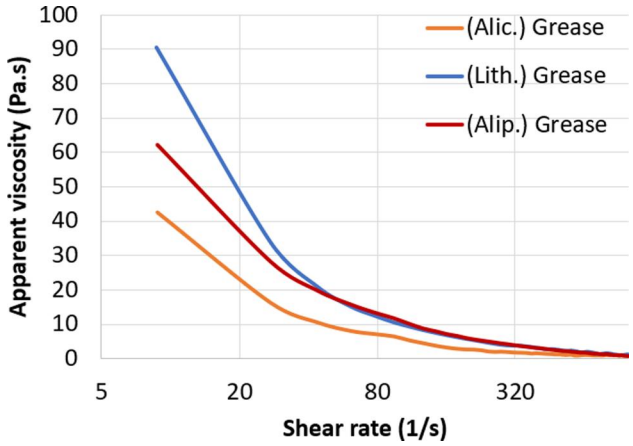

Figure 12. Apparent viscosity of tested greases.

Apparent viscosity measurement

Figure 12 shows the apparent viscosity results from a plate-plate rheometer. Measurements were taken at 24 °C at shear rates from 0.1 s^{-1} to 1000 s^{-1} with a gap of 1 mm. It can be seen that (Lith.) grease has the highest apparent viscosity in the low shear rate region. The (Alic.) grease shows the lowest apparent viscosity. The values from the (Lith. and Alip.)

measurements started to overlap from a shear rate of 60 (1/s). As the shear rate increased, all the apparent viscosities approached each other. Nevertheless, for the largest shear rate, the viscosity of (Alic.) grease was 20% less than that of (Lith. and Alip.). The differences in viscosity therefore does not explain the differences in measured film thicknesses for the various grease types.

Discussion

The current equation describing the contact film thickness in an axially loaded grease lubricated ball bearing is based on the product of base oil viscosity, contact width, and velocity (η b u), (*16*,*33*) see Eq. [1]. This is quite surprising since it was shown in Cen and Lugt (*16*) that the film thickness can be larger than the film thickness that would have been obtained with only base oil under fully flooded conditions. This suggests that the thickener may play a role in the formation of the film, even though the equation does not contain any thickener information. The equation was shown to work well for lithium, lithium complex and polyurea greases. Cen and Lugt (*16*) did not perform many measurements at very low speed, which could be the reason that this additional (thickener) effect was not found.

The measurements in this paper on the ball-on-disc and the full bearing dedicated to low speed, shows that the grease with the aliphatic di-urea (named Alip.) and lithium complex (named Lith.) thickeners again can be described with ηbu. However, the alicyclic di-urea grease clearly generates thicker films. Unfortunately, Cen and Lugt (*33*) did not report the type of polyurea thickener. It is therefore likely that the polyurea grease that they used was not an alicyclic di-urea.

The ball-on-disc experiments showed different thicknesses for tested samples where the thickness can be ranked with increasing values as alicyclic di-urea > aliphatic di-urea > lithium complex. This order applies for film thicknesses with fresh grease, grease that has been run in, and for a remaining film after stopping the test.

The viscosity of the alicyclic di-urea grease was lower than that of the other greases, which therefore cannot explain the increase in film thickness due to thickener. The difference is therefore ascribed to the ability of the thickener to adhere to the contact surfaces, i.e. to form thickener layers. More work is needed to confirm this.

The ball-on-disc experiments show that the (Alic.) grease behaves clearly differently from the (Lith.) and (Alip.) greases. The film thickness of (Alic.) initially reduces significantly but later increases again. Both (Lith.) and (Alp.) show a small decrease in film thickness over time. A decrease in film thickness is expected due to shear aging of the grease. Similar behavior was shown *via* experiments comparing fresh and mechanically aged grease by Cen et al. (*29*). The recovery of (Alic.), therefore, appears to be due to only the formation of a thickener boundary layer.

The formation of such layers can be explained by the fact that Alicyclic di-urea thickener (Alic.) shows less affinity for hydrocarbon base oils than aliphatic-di urea, and lithium complex thickeners. This effect could also lead to adherence to the surface and/or agglomeration of thickener material. A similar observation was made by Kaneta et al. (*25*) and Kanazawa et al. (*27*,*28*). However, the aforementioned studies only focus on short experiments and have been performed with different levels of starvation. The larger layer formation is best illustrated in the ball-on-disc tests where the rig is suddenly stopped Fig. 9 and where the thickness of the remaining lubricating film for (Alip.) and (Lith.) is approximately equal to the diameter of the thickener fibers but where the film of (Alic.) is much larger. Under these conditions, there appears to be a dominant effect of the thickener on the lubricating film. The effect was shown at higher speeds in the experiments presented in Fig. 3 where the film initially reduces, probably due to shear thinning, but later increases, an effect that can only be currently ascribed to the formation of a thickener layer.

Several properties of the grease have an impact on the film thickness development. The first is the size of the thickener agglomerates in the sample. Okal et al. (*38*) and Kostal et al. (*39*) showed that the alicyclic di-urea contains large agglomerates of thickener which increase the film thickness considerably in the initial hours of operation. However, during the first few minutes of the experiments, these agglomerates are gradually reduced due to high contact pressure and shear. The evolution of thickness is then not only determined by shear aging but also by the formation of a thickener layer, which is determined by the difference between thickener—base oil and thickener—steel surface affinity. This effect was observed at all tested speeds for the (Alic.) grease. Shear and pressure in the EHL contacts cause a demulsification of the thickener-oil system, separating the thickener and base oil, and the thickener forming a boundary layer on the surface(s). However, the growth of the thickener layer on the track is finite and stagnates after a certain time. The stagnation of the layer growth may be due to the increasing distance of the layer surface from the surface on which it is formed. As the distance increases, the attractive force of the surface will decrease. Another cause may be a reduction of layer strength with layer thickness. This statement is supported by the measurements in Figs. 3 and 4 where for three different velocities the profile of the increase was very similar.

Real ball bearing measurement

Figure 10 shows the results measured using the capacitance method on a ball bearing and Fig. 11 shows the normalized thickness with the prediction following the power relationship between normalized film thickness and the product of velocity, viscosity and contact width from Cen and Lugt. (*16*). Good agreement with the results from the optical tribometer at low velocities was observed. The reason for the agreement would be the fully flooded conditions that occurred in both cases. The low bearing speed caused sufficiently effective replenishment. The normalized film thickness for (Alip.) and (Lith.) is slightly lower than predicted

with the equation, possibly due to empirical limitations in the previously mentioned equation.

At higher speeds, (Lith., Alip.) greases showed a good agreement with the model curve. By contrast, (Alic.) grease, showed consistently thicker films, although the shape of the film thickness curve is very similar to the curve of the other samples. The reason is believed to be the formation of a thickener boundary layer that adhered to the surfaces. A greater influence of the thickener was also observed in the greater spread of the measured values for (Alic.) grease. The measurements were carried out for 24 h, which was long enough for the growth of this layer. The unexpected thicker film could not be explained by the rheology of the grease. The grease viscosity at low shear rates indicates an opposite effect. This suggest that the equation from Cen and Lugt (*33*) may not be valid for all greases.

The measurements were carried out at low operating speeds and at low bearing load. Higher speeds (higher shear) and longer operating times (more shear energy) may remove the thickener layer again. In the initial hours of operation and during the churning phase, the thickener layer is significantly higher than under "normal" operating conditions. After the grease reservoirs have formed and the bearing is operating in bleeding phase, the influence of the base oil, that is, viscosity will dominate. However, the thickener effect can be observed even after run-in Fig. 11b. When comparing Fig. 11a and b, slightly lower values can be observed for case Fig. 11b indicating that longer operation and bearing run-in may reduce the ability of the thickener to form a residual film on the raceways. This may be due to the higher shear stress, which will cause damage to the structure of the thickener. The same conclusions were found when studying fresh and mechanically aged grease (*29*).

Conclusions

To further expand the knowledge of lubricant film formation in grease-lubricated ball bearings, it is important to investigate how the individual lubricant components behave in EHL contacts. In this paper, several greases were tested using an optical tribometer and an actual ball bearing rig. The most important findings can be summarized in the following points:

- The film thickness trends in the ball-on-disc contact simulator compare well with those found in a real ball bearing using the electrical capacitance technique. Specifically, these trends can be observed at slow bearing speeds where fully flooded conditions occur.
- The power-law equation describing the thickness evolution in a ball bearing from Cen and Lugt (*16*) based on the ηbu parameters, requires refinement for the low-speed regime when the thickener properties also influence the film formation.
- The film thickness in a ball bearing using alicyclic di-urea shows higher values than predicted by the ηbu equation (*16*) throughout the low-speed regime ($10{,}000 < ndm < 60{,}000$ mm/min). The increase in film thickness was not due to the viscosity difference at low shear rates, but to the formation of a film thickener layer, which was also successfully observed on a ball-on-disc tribometer. The layer formation occurs in the first few hours of operation reaching a thickness of about 500–550 nm.
- For grease alicyclic di-urea, a greater film thickness was observed even after bearing break-in. At low speeds, grease particles with thickener and not just bled oil are involved in lubrication.
- The formation of the aforementioned thickener layer is related to the affinity of the thickener for the base oil PAO. The property of the thickener to bind to the contact surfaces appears to be another parameter needed to accurately predict the film thickness in a grease-lubricated ball bearing.
- The film thickness with the lithium complex and aliphatic di-urea shows slightly higher values than the model predicted at very low speeds but matches the model at higher speeds. At low speeds, there is good correlation between the ball-on-disc configuration tribometer and the real ball bearing.

The presented research has shown that the film thickness at low speed can be larger than predicted by the existing equation from Cen and Lugt (*16*). The equation from Cen and Lugt (*16*) does include the effect of the contribution of the thickener to the film thickness but assumes that this effect is grease-type independent. We have also shown here that there are greases that actually form even thicker films at low speed. We have shown here that this is most likely a function of the difference in affinity between thickener: base oil and thickener-surface material.

Acknowledgements

The ball-on-disc experiments were performed at Brno University of Technology and the bearing experiments were performed at the SKF University Technology Centre for Grease Lubrication at the University of Twente. We would like to thank SKF for agreeing to publish this work, as well as Dr. Kazumi Sakai and ENEOS Corporation for kindly preparing the samples.

Author contributions

All authors contributed to the study conception and design. Material preparation, data collection, and analysis were performed by M. Okal, D. Kostal, and P.M. Lugt. The first draft of the manuscript was written by M. Okal and all authors commented on previous versions of the manuscript. All authors read and approved the final manuscript.

Disclosure statement

No potential conflict of interest was reported by the author(s).

Funding

This research was carried out under the project FSI-S-23-8245 with financial support from the Ministry of Education, Youth and Sports of the Czech Republic.

ORCID

Michal Okal http://orcid.org/0000-0002-4833-6588
Piet M. Lugt http://orcid.org/0000-0001-9356-7599

References

(1) Hamrock, B. J. and Dowson, D. (1977), "Isothermal Elastohydrodynamic Lubrication of Point Contacts—Part III. Fully Flooded Results," *Journal of Lubrication Technology*, **99**, pp 264–276. doi:10.1115/1.3453074

(2) Nijenbanning, G., Venner, C. H., and Moes, H. (1994), "Film Thickness in Elastohydrodynamically Lubricated Elliptic Contacts," *Wear*, **176**, pp 217–229. doi:10.1016/0043-1648(94)90150-3

(3) Lugt, P. M. (2009), "A Review on Grease Lubrication in Rolling Bearings," *Tribology Transactions*, **52**, pp 470–480. doi:10.1080/10402000802687940

(4) Wikström, V. and Jacobson, B. (1997), "Loss of Lubricant from Oil-Lubricated Near-Starved Spherical Roller Bearings," *Proceedings of the Institution of Mechanical Engineers, Part J*, **211**, pp 51–66. doi:10.1243/1350650971542318

(5) Lugt, P. M., Holgerson, M., and Reinholdsson, F. (2023), "Impact of Oxidation on Grease Life in Rolling Bearings," *Tribology International*, **188**, 108785. doi:10.1016/j.triboint.2023.108785

(6) Wedeven, L. D., Evans, D., and Cameron, A. (1971), "Optical Analysis of Ball Bearing Starvation," *Journal of Lubrication Technology*, **93**, pp 349–361. doi:10.1115/1.3451591

(7) Kingsbury, E. (1985), "Parched Elastohydrodynamic Lubrication," *Journal of Tribology*, **107**, pp 229–232. doi:10.1115/1.3261026

(8) Chevalier, F., Lubrecht, A. A., Cann, P. M. E., Colin, F., and Dalmaz, G. (1998), "Film Thickness in Starved EHL Point Contacts," *Journal of Tribology*, **120**, pp 126–133. doi:10.1115/1.2834175

(9) Damiens, B., Venner, C. H., Cann, P. M., and Lubrecht, A. A. (2004), "Starved Lubrication of Elliptical EHD Contacts," *Journal of Tribology*, **126**, pp 105–111. doi:10.1115/1.1631020

(10) Venner, C. H., Berger, G., and Lugt, P. M. (2004), "Waviness Deformation in Starved EHL Circular Contacts," *Journal of Tribology*, **126**, pp 248–257. doi:10.1115/1.1572514

(11) Svoboda, P., Kostal, D., Krupka, I., and Hartl, M. (2013), "Experimental Study of Starved EHL Contacts Based on Thickness of Oil Layer in the Contact Inlet," *Tribology International*, **67**, pp 140–145. doi:10.1016/j.triboint.2013.07.019

(12) Van Zoelen, M. T., Venner, C. H., and Lugt, P. M. (2010), "Free Surface Thin Layer Flow in Bearings Induced by Centrifugal Effects," *Tribology Transactions*, **53**, pp 297–307. doi:10.1080/10402000903283284

(13) Jablonka, K., Glovnea, R., and Bongaerts, J. (2012), "Evaluation of EHD Films by Electrical Capacitance," *Journal of Physics D: Applied Physics*, **45**, 385301. doi:10.1088/0022-3727/45/38/385301

(14) Bader, N., Furtmann, A., Tischmacher, H., Poll, G. (2017), Capacitances and Lubricant Film Thicknesses of Grease and Oil Lubricated Bearings," *Proceedings of the STLE Annual Meeting & Exhibition*, Atlanta, GA, Volume 72, pp 311–314.

(15) Zhang, X. and Glovnea, R. (2021), "Grease Film Thickness Measurement in Rolling Bearing Contacts," *Proceedings of the Institution of Mechanical Engineers, Part J*, **235**, pp 1430–1439. doi:10.1177/1350650120961278

(16) Cen, H. and Lugt, P. M. (2020), "Replenishment of the EHL Contacts in a Grease Lubricated Ball Bearing," *Tribology International*, **146**, 106064. doi:10.1016/j.triboint.2019.106064

(17) Cen, H., Lugt, P. M., and Morales-Espejel, G. (2014), "On the Film Thickness of Grease-Lubricated Contacts at Low Speeds," *Tribology Transactions*, **57**, pp 668–678. doi:10.1080/10402004.2014.897781

(18) Cen, H. and Lugt, P. M. (2021), "Effect of Start-Stop Motion on Contact Replenishment in a Grease Lubricated Deep Groove Ball Bearing," *Tribology International*, **157**, 106882. doi:10.1016/j.triboint.2021.106882

(19) Shetty, P., Meijer, R. J., Osara, J. A., and Lugt, P. M. (2022), "Measuring Film Thickness in Starved Grease-Lubricated Ball Bearings: An Improved Electrical Capacitance Method," *Tribology Transactions*, **65**, pp 869–879. doi:10.1080/10402004.2022.2091067

(20) Shetty, P., Meijer, R. J., Osara, J. A., Pasaribu, R., and Lugt, P. M. (2024), "Vibrations and Film Thickness in Grease-Lubricated Deep Groove Ball Bearings," *Tribology International*, **193**, 109325. doi:10.1016/j.triboint.2024.109325

(21) Shetty, P., Meijer, R. J., Osara, J. A., Pasaribu, R., and Lugt, P. M. (2024), "Effect of Grease Filling on the Film Thickness in Deep-Groove Ball Bearings," *Tribology Transactions*, **67**, pp 62–69. doi:10.1080/10402004.2023.2282632

(22) Cann, P. M. (1999), "Starved Grease Lubrication of Rolling Contacts," *Tribology Transactions*, **42**, pp 867–873. doi:10.1080/10402009908982294

(23) Cann, P. M. (1996), "Starvation and Reflow in a Grease-Lubricated Elastohydrodynamic Contact," *Tribology Transactions*, **39**, pp 698–704. doi:10.1080/10402009608983585

(24) Cann, P. M. (2007), "Grease Lubrication of Rolling Element Bearings—Role of the Grease Thickener," *Lubrication Science*, **19**, pp 183–196. doi:10.1002/ls.39

(25) Kaneta, M., Ogata, T., Takubo, Y., and Naka, M. (2000), "Effects of a Thickener Structure on Grease Elastohydrodynamic Lubrication Films," *Proceedings of the Institution of Mechanical Engineers, Part J*, **214**, pp 327–336. doi:10.1243/1350650001543214

(26) Hoshi, Y., Takiwatari, K., Nanao, H., and Mori, S. (2020), "In Situ Observation of Transient Responses in Grease Lubrication by Micro Infrared Spectroscopy," *Tribology Online*, **15**, pp 201–208. doi:10.2474/trol.15.201

(27) Kanazawa, Y., De Laurentis, N., and Kadiric, A. (2020), "Studies of Friction in Grease-Lubricated Rolling Bearings Using Ball-on-Disc and Full Bearing Tests," *Tribology Transactions*, **63**, pp 77–89. doi:10.1080/10402004.2019.1662147

(28) Kanazawa, Y., Sayles, R. S., and Kadiric, A. (2017), "Film Formation and Friction in Grease Lubricated Rolling-Sliding Non-Conformal Contacts," *Tribology International*, **109**, pp 505–518. doi:10.1016/j.triboint.2017.01.026

(29) Cen, H., Lugt, P. M., and Morales-Espejel, G. (2014), "Film Thickness of Mechanically Worked Lubricating Grease at Very Low Speeds," *Tribology Transactions*, **57**, pp 1066–1071. doi:10.1080/10402004.2014.933936

(30) Hartl, M., Křupka, I., Poliščuk, R., and Liška, M. (1999), "An Automatic System for Real-Time Evaluation of EHD Film Thickness and Shape Based on the Colorimetric Interferometry," *Tribology Transactions*, **42**, pp 303–309. doi:10.1080/10402009908982221

(31) Hartl, M., Krupka, I., Poliscuk, R., Liska, M., Molimard, J., Querry, M., and Vergne, P. (2001), "Thin Film Colorimetric Interferometry," *Tribology Transactions*, **44**, pp 270–276. doi:10.1080/10402000108982458

(32) Heemskerk, R. S., Vermeiren, K. N., and Dolfsma, H. (1982), "Measurement of Lubrication Condition in Rolling Element Bearings," *ASLE Transactions*, **25**, pp 519–527. doi:10.1080/05698198208983121

(33) Cen, H. and Lugt, P. M. (2019), "Film Thickness in a Grease Lubricated Ball Bearing," *Tribology International*, **134**, pp 26–35. doi:10.1016/j.triboint.2019.01.032

(34) Wilson, A. R. (1979), "The Relative Thickness of Grease and Oil Films in Rolling Bearings," *Proceedings of the Institution of Mechanical Engineers*, **193**, pp 185–192. doi:10.1243/PIME_PROC_1979_193_019_02

(35) Hamrock, B. J. and Dowson, D. (1977), "Isothermal Elastohydrodynamic Lubrication of Point Contacts. Part 4—

Starvation Results," *Journal of Lubrication Technology*, **99**, pp 15–23. doi:10.1115/1.3452973

(36) DIN Deutsches Institut für Normung e.V. DIN 51817. (2014), *Testing of Lubricants—Determination of Oil Separation from Greases Under Static Conditions*, Beuth Verlag GmbH: Berlin, Germany.

(37) "SKF Rolling Bearings Catalogue 17000" (2018). AB SKF: Gothenburg, Sweden.

(38) Okal, M., Kostal, D., Sakai, K., Krupka, I., and Hartl, M. (2024), "Thickener Behaviour in Rolling Elastohydrodynamic Lubrication Contacts," *Tribology Letters*, **72**, 72. doi:10.1007/s11249-024-01874-0

(39) Kostal, D., Okal, M., Fryza, J., Krupka, I., and Hartl, M. (2022), "Novel In-Situ Observation of the Grease Constituents in Elastohydrodynamic Contacts by Fluorescence Microscopy," *Tribology Letters*, **70**, 126. doi:10.1007/s11249-022-01671-7